The Journal of Immunology

SARS-CoV-2 Neutralizing Antibody Responses towards Full-Length Spike Protein and the Receptor-Binding Domain

Rafael Bayarri-Olmos, Manja Idorn, Anne Rosbjerg, Laura Pérez-Alós, Cecilie Bo Hansen, Laust Bruun Johnsen, Charlotte Helgstrand, Franziska Zosel, Jais Rose Bjelke, Fredrik Kryh Öberg, Max Søgaard, Søren R. Paludan, Theresa Bak-Thomsen, Joseph G. Jardine, Mikkel-Ole Skjoedt and Peter Garred

J Immunol 2021; 207:878-887; Prepublished online 23 July 2021;
doi: 10.4049/jimmunol.2100272
http://www.jimmunol.org/content/207/3/878

The Journal of Immunology is published twice each month by
The American Association of Immunologists, Inc.,
1451 Rockville Pike, Suite 650, Rockville, MD 20852

Print ISSN: 0022-1767 Online ISSN: 1550-6606.

SARS-CoV-2 Neutralizing Antibody Responses towards Full-Length Spike Protein and the Receptor-Binding Domain

Rafael Bayarri-Olmos,* Manja Idorn,† Anne Rosbjerg,* Laura Pérez-Alós,* Cecilie Bo Hansen,* Laust Bruun Johnsen,‡ Charlotte Helgstrand,‡ Franziska Zosel,‡ Jais Rose Bjelke,‡ Fredrik Kryh Öberg,‡ Max Søgaard,§ Søren R. Paludan,† Theresa Bak-Thomsen,‡ Joseph G. Jardine,¶ Mikkel-Ole Skjoedt,*,[1] and Peter Garred*,[1]

Tools to monitor SARS-CoV-2 transmission and immune responses are needed. We present a neutralization ELISA to determine the levels of Ab-mediated virus neutralization and a preclinical model of focused immunization strategy. The ELISA is strongly correlated with the elaborate plaque reduction neutralization test (ρ = 0.9231, $p < 0.0001$). The neutralization potency of convalescent sera strongly correlates to IgG titers against SARS-CoV-2 receptor-binding domain (RBD) and spike (ρ = 0.8291 and 0.8297, respectively; $p < 0.0001$) and to a lesser extent with the IgG titers against protein N (ρ = 0.6471, $p < 0.0001$). The preclinical vaccine NMRI mice models using RBD and full-length spike Ag as immunogens show a profound Ab neutralization capacity (IC_{50} = 1.9 × 10^4 to 2.6 × 10^4 and 3.9 × 10^3 to 5.2 × 10^3, respectively). Using a panel of novel high-affinity murine mAbs, we also show that a majority of the RBD-raised mAbs have inhibitory properties, whereas only a few of the spike-raised mAbs do. The ELISA-based viral neutralization test offers a time- and cost-effective alternative to the plaque reduction neutralization test. The immunization results indicate that vaccine strategies focused only on the RBD region may have advantages compared with the full spike. *The Journal of Immunology*, **2021, 207: 878–887.**

Coronavirus disease-19 has, within a short time, become a worldwide health crisis and the scientific community has stepped up in earnest to this unprecedented challenge to develop diagnostic and therapeutic tools to contain and treat the pandemic. As of September 2020, there were 231 vaccine candidates in the pipeline and more than 30 in clinical trials (1). December 2020 saw the rollout of mass vaccination programs around the globe, and by the end of February 2021, more than 175 million doses had been administered from at least seven different approved vaccines (2). Apart from vaccines to prevent SARS-CoV-2 infection, passive anti–SARS-CoV-2 Ab therapy to treat COVID-19 patients has emerged as a treatment possibility (3). Studies have reported that the majority of COVID-19 patients develop neutralizing Abs targeting the spike glycoprotein within the first 2 wk after symptom onset (4–8), and that SARS-CoV-2–derived Abs have a protective effect in COVID-19 animal models such as rhesus macaques (9) and rodents (10–13). The U.S. Food and Drug Administration has granted Emergency Use Authorizations to two combination products, bamlanivimab plus etesevimab (two mAbs with overlapping epitopes in the receptor-binding domain [RBD] of the spike protein) and casirivimab plus imdevimab (previously REGN10933 and REGN10987, respectively, which target nonoverlapping epitopes in the RBD), for the treatment of outpatients with mild to moderate COVID-19 at risk for developing severe disease and/or requiring hospitalization (14). Overall, current reports support the idea that Ab-based immunotherapy in the form of mAbs is beneficial in the treatment of COVID-19 patients. At the same time, the use of convalescent plasma therapy has become debated (15–17). Nevertheless, protective humoral immunity involves neutralizing Abs and will be a hallmark for the evaluation of a vaccine response efficacy.

The current standard method to evaluate the presence of neutralizing Abs in the blood is the plaque reduction neutralization test (PRNT). Although it remains the gold standard because of its specificity and sensitivity (18–21), the PRNT is labor and time intensive, difficult to standardize, and requires highly specialized personnel in high biosafety levels laboratories. Alternatively, viral particles pseudotyped with SARS-CoV-2 spike have been developed and allow for faster and safer determination of Ab-mediated neutralization

*Copenhagen University Hospital, Copenhagen, Denmark; †Department of Biomedicine, Aarhus Research Center for Innate Immunology, Aarhus University, Aarhus, Denmark; ‡Novo Nordisk, Måløv, Denmark; §Neutralizing Antibody Center, Scripps Research, International AIDS Vaccine Initiative, La Jolla, CA; and ¶ExpreS2ion Biotechnologies, Horsholm, Denmark

[1]M.-O.S. and P.G. contributed equally to this work.

ORCIDs: 0000-0003-3202-9679 (R.B.-O.); 0000-0002-6769-9165 (M.I.); 0000-0001-6736-3138 (A.R.); 0000-0002-0368-4976 (L.P.-A.); 0000-0002-7709-4522 (C.B.H.); 0000-0002-8496-3423 (C.H.); 0000-0002-5137-6601 (F.Z.); 0000-0002-7089-2118 (F.K.Ö.); 0000-0001-6224-4818 (M.S.); 0000-0001-8951-1074 (J.G.J.); 0000-0003-1306-6482 (M.-O.S.); and 0000-0002-2876-8586 (P.G.).

Received for publication March 23, 2021. Accepted for publication June 2, 2021.

This work was supported by grants from the Carlsberg Foundation (CF20-0045), the Novo Nordisk Foundation (NFF205A0063505 and NNF20SA0064201), and the Independent Research Fund Denmark (0214-00001B).

R.B.-O., M.-O.S., and P.G. conceived and designed the study; R.B.-O., C.H., J.R.B., F.K.Ö., M.S., T.B.-T., and J.G.J. enabled recombinant protein production; R.B.-O. developed the ELISA-based neutralization assay; R.B.-O., L.P.-A., and C.B.H. performed the ELISA-based experiments; R.B.-O., A.R., and M.-O.S. generated and characterized the mAbs; C.B.H. enabled blood sample collection and use; M.I. and S.R.P. performed viral neutralization experiments; L.B.J. characterized Ab affinities and epitope mapping by BLI; F.Z. performed size exclusion chromatography coupled to multiangle light scattering (SEC-MALS) experiments; R.B.-O., M.I., L.P.-A., L.B.J., and S.R.P. analyzed the data; R.B.-O., M.-O.S., and P.G. wrote the paper with inputs from all coauthors. All authors approved the final version of the manuscript.

Address correspondence and reprint requests to Dr. Rafael Bayarri-Olmos, Laboratory of Molecular Medicine, Department of Clinical Immunology 7631, Copenhagen University Hospital Ole Maaloesvej 26, Entrance 76, 3rd Floor, 2200 Copenhagen, Denmark. E-mail address: rafael.bayarri.olmos@regionh.dk

The online version of this article contains supplemental material.

Abbreviations used in this article: ADE, Ab-dependent enhancement; AMC, anti-mouse IgG Fc capture; BLI, biolayer interferometry; CV, coefficient of variation; HS-strep-HRP, high-sensitivity streptavidin–HRP; IAVI, International AIDS Vaccine Initiative; PRNT, plaque reduction neutralization test; RBD, receptor-binding domain; RT, room temperature; SEC-MALS, size exclusion chromatography coupled to multiangle light scattering.

(22–26). Notwithstanding, it remains of critical importance to develop reliable and convenient methods to assess the virus-neutralizing capacity of patient- or animal-derived Abs to select convalescent plasma donors, develop mAb-based therapeutics, and evaluate the efficacy of vaccination strategies.

In this study, we describe the development of a quick, sensitive, and easy-to-operate neutralization ELISA-based test for the determination of neutralizing Abs based on the interaction between recombinant human ACE-2 ectodomain and the SARS-CoV-2 RBD. We benchmarked our assay with the PRNT and two commercially available tests. Using a previously described cohort of PCR-confirmed COVID-19 convalescent patients (27), we measured the neutralization potency and the relative titers of IgG, IgM, and IgA against the RBD, spike, and protein N. Furthermore, we evaluated the vaccine responses in preclinical vaccine animal models using our Ab neutralization ELISA and generated high-affinity mAbs against the RBD and full-length spike protein. Finally, we performed binding kinetic characterization, epitope binning, and determined their neutralization potency in our Ab neutralization ELISA and the PRNT.

Materials and Methods

Buffers

The following buffers were used: PBS (10.1 mM disodium phosphate, 1.5 mM monopotassium phosphate, 2.7 mM potassium chloride, 137 mM sodium chloride), PBS-T (PBS + 0.05% Tween-20), PBS-T–EDTA (PBS-T + 5 mM EDTA), sample buffer (PBS-T–EDTA + 5% skim milk [70166 Merck, Branchburg, NJ]).

Production and purification of recombinant ACE-2 ectodomain and SARS-CoV-2 viral proteins

The nucleotide sequence corresponding to the human ACE-2 receptor (aa 17–740) with an N-terminal CD33 signal peptide and a dual C-terminal 10xHis-AviTag (HHHHHHHHHH-GLNDIFEAQKIEWHE) was ordered from Twist Biosciences and subcloned into a pTT5 expression vector. Recombinant ACE-2 protein was produced by transient transfection using the Expi293 Expression System Kit (Life Technologies, Thermo Fisher Scientific, Waltham, MA) according to the manufacturer's recommendations and grown shaking in suspension in a humidified incubator at 37°C and 8% CO_2. On day 5 after transfection, AmMag Ni Magnetic Beads (GenScript, Piscataway, NJ) or IMAC-5 MAG magnetic beads (Lytic solutions, Madison, Wisconsin) were added to the clarified cell culture, followed by 2 h of additional incubation. The magnetic beads were subsequently removed from the cell culture, washed, and eluted according to the manufacturer's instructions. The two elutions were pooled, and buffer exchanged into 50 mM HEPES (pH 7.4), 150 mM NaCl. The nucleotide sequence for the trimeric prefusion-stabilized spike protein ectodomain (QIC53204, aa 1–1208) was optimized in terms of the codon adaptation index, high 5' mRNA folding energy, and repeated adjacent codons. The coding sequence was modified by including two stabilizing proline substitutions in positions 986–987, a GSAS substitution at the furin cleavage site (aa 682–685), and a C-terminal trimerization domain-8xHis (YIPEAPRDGQAYVRKDGEWVLLSTFL-HHHHHHHH) (28). All DNA manipulations were done in Visual Gene Developer 1.9 (29). The nucleotide sequence was synthesized by GeneArt (Thermo Fisher Scientific) and subcloned into a pcDNA3.4 expression vector. Trimeric prefusion-stabilized spike protein ectodomain was produced and purified as were SARS-CoV-2 protein N and RBD, which have been described in detail elsewhere (27). Purified RBD was biotinylated with a biotin ligase kit (Avidity, Aurora, Colorado, USA) according to the manufacturer's instructions. The plasmid used for synthesizing the SARS-CoV-2 RBD polypeptide was made and kindly contributed by the International AIDS Vaccine Initiative and provided by the responsible International AIDS Vaccine Initiative employee, Joseph Jardine (Scripps Institute, La Jolla, California). The nucleotide sequence for the monomeric prefusion-stabilized spike protein ectodomain (aa 16–1208), modified with an N-terminal BiP signal peptide, two proline substitutions (aa 967, 987) an AARA substitution at the furin cleavage site, and a C-terminal Capture select C-tag (Thermo Fisher Scientific), was synthesized and subcloned into a pExpreS2-1 (ExpreS^{2}ion Biotechnologies) vector by GeneArt. Transiently transfected *Drosophila melanogaster* S2 cells (ExpreS^2 Cells, ExpreS^{2}ion Biotechnologies) were grown shaking in suspension at 25°C for 3 d after which the supernatant was harvested by centrifugation, concentrated, and buffer exchanged ~10-fold. The protein was purified on a Capture Select C-tag XL column (Thermo Fisher Scientific) eluted using $MgCl_2$ (0.5–1 M), followed by size exclusion chromatography using a Superdex200 column (Cytiva, Marlborough, MA) equilibrated in PBS.

Protein purity was confirmed by SDS gel electrophoresis using a Tris-Acetate 3–8% gel (Invitrogen, Thermo Fisher Scientific) and Instant Blue total protein stain (Abcam, Cambridge, UK), and the identity of the purified proteins was confirmed using Bis-Tris 4–12% gels blotted unto Invitrolon PVDF membranes (both Invitrogen, Thermo Fisher Scientific) and detecting either with anti-human ACE-2 goat IgG (AF933; R&D Systems, Minneapolis, MN) followed by anti-sheep–HRP conjugate polyclonal rabbit 1.3 g/L (P0163 Dako; Agilent, La Jolla,CA) or with streptavidin-HRP conjugate (RPN131V; Amersham, Sigma-Aldrich, St. Louis, MO).

Characterization of RBD and spike protein by size exclusion chromatography coupled to multiangle light scattering

A total of 30 μg (RBD) or 20 μg (spike protein) of protein were injected on an HPLC system (Alliance; Waters, Milford, MA) and separated on a Superose 6 increase 10/300 GL column (Cytiva) equilibrated with 20 mM HEPES (pH 7.5), 150 mM NaCl at a flow rate of 0.5 ml/min. Eluting sample was detected with light scattering (miniDAWN Treos; Wyatt Technologies, Goletta, CA), RI (Optilab rEX; Wyatt Technologies), and UV detectors. The light scattering data were analyzed in Astra (Wyatt Technologies), assuming a refractive index increment of 0.185 ml/g.

Serum and plasma samples

A total of 310 serum and plasma samples from recovered individuals with a previous SARS-CoV-2 infection confirmed by quantitative PCR were included in the study. The participants have been described elsewhere (27). Serum and plasma samples from healthy blood donors collected before December 2019 were used as negative control.

Development of an ELISA-based SARS-CoV-2 neutralization assay

The assay was optimized by sequentially assessing the effect of detection reagents, (i.e., high-sensitivity streptavidin–HRP [HS-strep-HRP; 21130; Thermo Fisher Scientific] or streptavidin-HRP conjugate [RPN131V; Amersham]; convalescent serum preincubation times [0–60 min]; ACE-2 coat concentration [0.5–8 μg/ml]; RBD:ACE-2 binding times [15–90 min]; and sample choice [serum, heat-inactivated serum, plasma]). In the final setup, ACE-2 (1 μg/ml) was coated in MaxiSorp microtiter plates (Thermo Fisher Scientific) overnight in PBS at 4°C. The day after, biotinylated RBD (4 ng/ml) was incubated with HS-strep-HRP (1:16,000 dilution) and convalescent serum dilutions (6-point 4-fold dilution starting at 20%) for 60 min in low-binding polypropylene round-bottom plates (Thermo Fisher Scientific). Next, the serum/RBD mix was transferred to ACE-2 coated plates and allowed to bind for 15 min, before detection with TMB ONE (KemEnTec Diagnostics, Taastrup, Denmark). The reaction was stopped with 0.3 M H_2SO_4, and the OD was measured at 450 nm. Microtiter plates were washed thrice with PBS-T between steps and all incubations took place at room temperature (RT) in an orbital shaker unless otherwise stated. The neutralization index was calculated as:

$$\text{Neutralization } (\%) = \left(1 - \frac{\text{sample OD}}{\text{control OD}}\right) \times 100$$

Negative neutralization indexes were normalized to 0. A serum pool (n = 3) collected before the emergence of SARS-CoV-2 was used as control. The matrix effects are represented as the ratio between each dilution of serum/plasma/nonspecific mAbs and the blank (RBD/HS-strep-HRP ratio in PBS-T) × 100. The intra-assay coefficient of variation (CV) was calculated on the estimated IC_{50} values of a serum pool from six convalescent patients with high anti-RBD IgG titers measured eight times in a single plate. The interassay CV was calculated on the average IC_{50} of a serum sample with high anti-RBD IgG titers from at least three independent plates run in three different days (n = 12–15).

PRNT

SARS-CoV-2, Freiburg isolate, and FR-4286 (kindly provided by Professor Georg Kochs, University of Freiburg) was propagated in VeroE6 cells expressing human TMPRSS2 (VeroE6-hTMPRSS2) [kindly provided by Professor Stefan Pöhlmann, University of Göttingen (30)] with a multiplicity of infection of 0.05 in DMEM (Life Technologies, Thermo Fisher Scientific) + 2% FCS (Sigma-Aldrich) + 1% penicillin/streptomycin (Life Technologies) + L-glutamine (Sigma-Aldrich) (in this study, complete medium). Supernatant from 72 h postinfection containing new virus progeny was harvested and concentrated on 100 kDa Amicon ultrafiltration columns (Merck) by centrifugation at 4,000 × g for 30 min. Virus titer was determined by the 50% tissue culture infectious dose assay and calculated by Reed-Muench method (31). Sera from convalescent COVID-19 patients (15 representative samples with low, intermediate, and high RBD-specific IgG titers) was heat-inactivated (30

min, 56°C), and prepared in 2-fold serial dilutions in complete medium. MAbs raised against SARS-CoV-2 RBD, or prefusion-stabilized spike protein were prepared in complete medium at 100 μg/ml and subsequent 3-fold serial dilution. Serum or Ab dilutions were mixed with SARS-CoV-2 at a final titer of 100 the 50% tissue culture infectious dose per well and incubated at 4°C overnight. "No serum" and "no virus" (uninfected) samples were included as controls. The following day, virus/serum or virus/Ab mixtures were added to 2×10^4 Vero E6-hTMPRSS2 cells seeded in flat-bottom 96-well plates, and incubated for 72 h in a humidified CO_2 incubator at 37°C, 5% CO_2. The neutralization assay was stopped by fixing with 5% Formalin (Sigma-Aldrich) and staining with crystal violet solution (Sigma-Aldrich). The plates were read using a light microscope (Leica DMi1, Leica, Wetzlar, Germany) with a camera (Leica MC170 HD) at 10× magnification, and the cytopathic effect scored.

Determination of IgG, IgM, and IgA titers against RBD, spike, and protein N

Microtiter 384-well plates were coated with 1 μg/ml of RBD, monomeric full-length spike, or protein N in PBS overnight at 4°C. Serum samples from COVID-19 convalescent patients were applied in a 3-point 3-fold serial dilution starting at 1:400 in sample buffer. A serum sample from a COVID-19 patient with high IgG, IgM, and IgA titers against RBD was used as a calibrator. HRP-conjugated polyclonal rabbit Abs against human IgG (P0214), IgM (P0215), and IgA (P0216) (0.5 μg/ml; all from Agilent Technologies, Santa Clara, CA) were used as detection Abs. Unless otherwise stated, all incubation steps were performed for 1 h at RT in a shaking platform, and the plates were washed between steps with PBS-T. Plates were developed with TMB ONE for 7 min for IgG, and 10 min for IgM and IgA, and the reaction was stopped with 0.3 M H_2SO_4, and the OD was measured as described previously. Ab titers against RBD have previously been reported by our group (27).

Mice immunization and generation of mAbs against SARS-CoV-2 RBD and spike protein

Four groups ($n = 4$ per group) of outbred NMRI mice were immunized against SARS-CoV-2 RBD or trimeric prefusion-stabilized spike protein ectodomain. The mice used for mAb generation (two groups of four mice) received three s.c. injections with 20 μg of either recombinant RBD or trimeric prefusion-stabilized spike protein ectodomain adsorbed to GERBU P adjuvant (Gerbu, Heilderberg, Germany) as recommended by the manufacturer. The three rounds of immunization were spaced 2 wk apart. Four days before the fusions, the mice received an i.v. boost of 15 μg Ag without adjuvant. Splenocytes were collected and the fusion was done essentially as described previously (32). Hybridomas were screened by direct ELISA using MaxiSorp microtiter plates (Thermo Fisher Scientific) coated with 0.5 μg/ml of recombinant monomeric full-length spike protein or RBD and cloned by limiting dilution. Positive clones were purified with HiTrap Protein G columns connected to an Äkta Pure system (both from Cytiva).

For the preclinical vaccine strategy, the two other groups ($n = 4$) of mice received in total four doses of 20 μg of recombinant RBD or trimeric full-length spike protein ectodomain as above, and polyclonal antisera were collected 7 d after each immunization.

Determination of Ab titers in immunized mice and COVID-19 convalescent patients

Mice sera were applied to microtiter plates coated with RBD or monomeric full-length spike protein (both 1 μg/ml) in a 9-point 4-fold serial dilution starting at 1:100. Human convalescent sera were applied in an 8-point 4-fold serial dilution starting at 1:25. The samples were incubated for 80 min, followed by a 45-min incubation with rabbit anti-mouse-HRP conjugate (1:2000 dilution, P0260) or polyclonal rabbit Abs against human IgG (0.5 μg/ml, P0214) (both from Agilent Technologies). Development was performed as described previously.

Evaluation of the neutralization potency of mouse serum and mouse-derived mAbs

The neutralization potency was calculated on a 9-point 4-fold serial dilution of serum (starting at a 1:40 dilution) or a 6-point 4-fold dilution of purified mAbs (starting at 24 μg/ml), but otherwise, as described before. Plates were washed between steps with PBS-T, and all incubations took place at RT.

Epitope binning and affinity determination of RBD and spike mAbs by biolayer interferometry

Binning experiments were performed using an Octet system (HTX, Red384) (ForteBio, Fremont, CA), based on the principle of biolayer interferometry (BLI), equipped with anti-mouse IgG Fc capture (AMC) sensors (Pall Life Sciences, San Diego, CA) and using the 8-channel mode. The binning assays were performed using a sandwich setup, and tips were regenerated between each cycle. Abs were captured directly from supernatants. Briefly (1), Abs were loaded on AMC tips (150 s) (2); AMC tips were blocked with 2 μM of a mix of mouse IgG2a, IgG2b, and IgG1 (300 s) (3); association with 100 nM spike protein (150 s); and (4) competition with second Abs (150 s). Unspecific binding was evaluated by including a mouse IgG1 Ab as a first and second Ab control. Response values from the second Abs from step (4) were used as the basis for the binning data, in addition to visual inspection of individual binding curves for all Ab competitions. Running/neutralization buffer was composed of 20 mM HEPES, 150 mM NaCl, 5 mM $CaCl_2$, 0.1% BSA (IgG free), 0.03% Tween-20 (pH 7.4). Regeneration buffer was 10 mM glycine-HCl (pH 1.5).

Affinity determination experiments were performed on the same Octet Fortebio System instrument as used for the binning experiment. Briefly (1), Abs were captured directly from supernatant on AMC sensors (150 s) (2), association to serial dilutions of RBD (10-point 2-fold dilution starting at 200 nM) (300 s), and (3) a dissociation phase (300 s). Reference AMC sensors, loaded with the same specific Abs as subjected to the RBD concentrations series, were subtracted for each specific Ab before data analysis. Global analysis of association and dissociation phases fitted to a 1:1 binding model were employed.

Statistics

All analyses were performed with GraphPad Prism 8 (GraphPad Software, San Diego, CA). IC_{50} values were calculated using the equation [inhibitor] versus normalized response with variable slope. IC_{50} values from nonneutralizing serum samples were normalized to 1, and mAbs were normalized to 100. The relationship between serum and plasma neutralization index, PRNT versus Ab neutralization ELISA log(IC_{50}), neutralization versus IgG/M/A titers, and neutralization versus RBD affinity was estimated by linear regression analyses (goodness of fit reported as R^2) and two-tailed Spearman rank correlation tests. IgG, IgM, and IgA titers were interpolated from a calibrator curve using a four-parameter nonlinear curve fitting and reported as arbitrary units/ml as described elsewhere (27). The p values < 0.05 were considered statistically significant.

Study approval

The use of convalescent donor blood sample in this study has been approved by the Regional Ethical Committee of the Capital Region of Denmark with the approval ID: H-20028627.

The animal experimental procedures described in this study have been approved by the Danish Animal Experiments Inspectorate with the approval ID: 2019-15-0201-00090.

Results

Development of an ELISA-based Ab neutralization test

We synthesized recombinant human ACE-2 ectodomain (aa 17–740), trimeric-stabilized spike ectodomain (aa 1–1208), and SARS-CoV-2 RBD (aa 319–591) and purified them by immobilized metal ion chromatography via their C-terminal 10xHis followed by size exclusion chromatography (Fig. 1A). To avoid steric hindrance between RBD-bound, nonneutralizing Abs in the analyte and detection Abs when determining the interaction between ACE-2 and RBD, we biotinylated the latter via a C-terminal AviTag (Fig. 1B, 1C). SEC-MALS analyses of RBD and spike protein ectodomain demonstrate that they behave as a 39-kDa monomer and a 530-kDa trimer in solution, respectively (Fig. 1D).

Using the recombinant ACE-2 ectodomain and biotinylated SARS-CoV-2 RBD, we developed an ELISA-based neutralization assay defining the reduction of the binding of RBD to coated ACE-2 as a measure for the neutralization potency of sera from convalescent patients or vaccinated mice (Fig. 1E). Aiming at making this assay as flexible and applicable by other laboratories and testing platforms, we screened the effects of the detection reagents, coat density, assay time, sample matrix, and sample type (Fig. 2). Briefly, the ACE-2 coat was titrated and evaluated in terms of the signal-to-noise ratio and total intensity, and a low-density coat of 1 μg/ml was used for further assay development (Fig. 2A). Shortening the RBD/ACE-2 ratio incubation time to 15 min resulted in the best signal-to-noise ratio, mostly because of a reduction in the

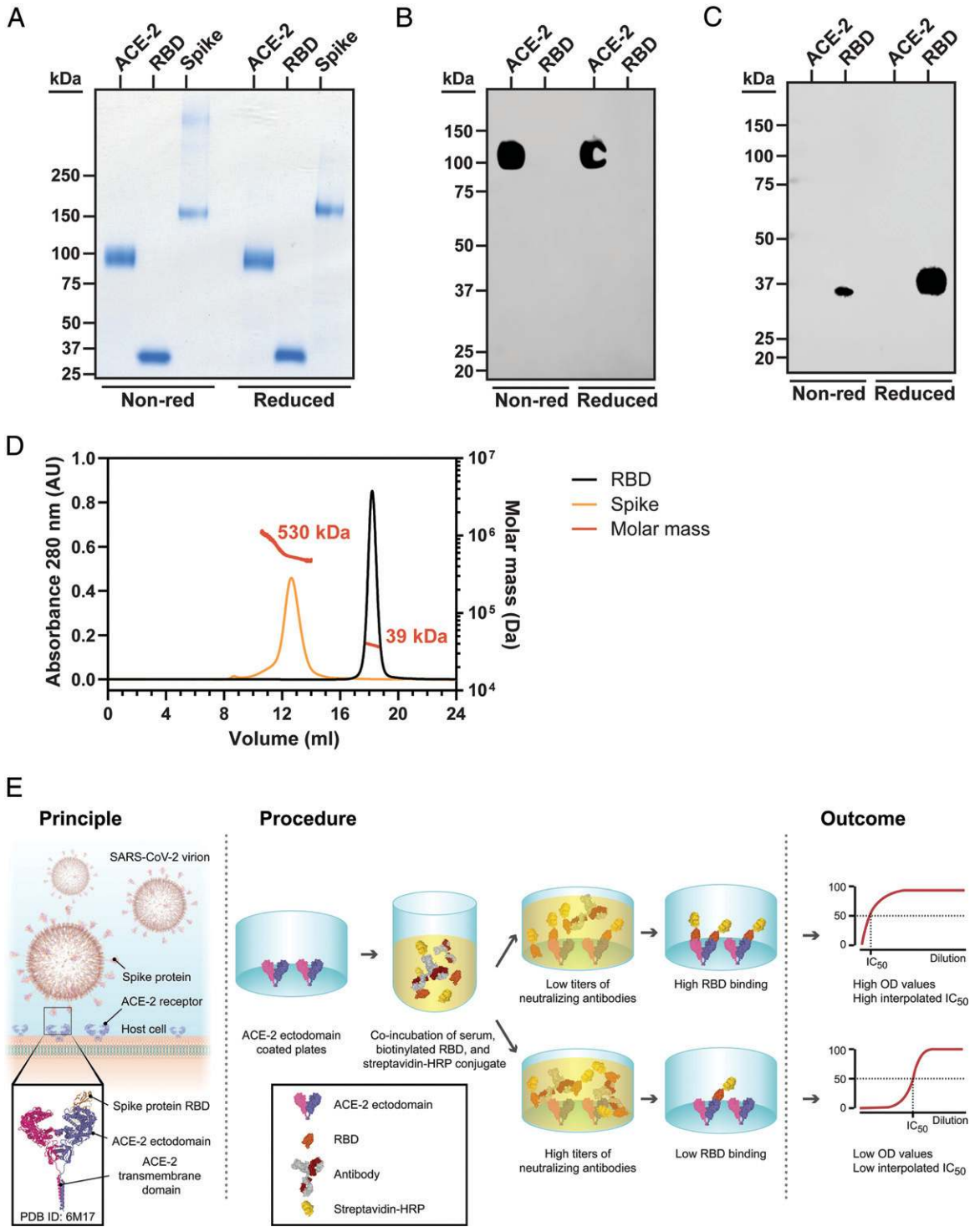

FIGURE 1. Production of recombinant human ACE-2 and SARS-CoV-2 RBD. Total protein stain of SDS-PAGE of purified ACE-2, trimeric spike and biotinylated RBD produced in Expi293 cells (**A**). Western immunoblotting using an anti–ACE-2 Ab (**B**), or streptavidin-HRP conjugate (**C**) of the ACE-2 and biotinylated RBD used in the Ab neutralization assay. SEC-MALS chromatograms of RBD (black) and spike protein (yellow) (**D**). The molar mass calculate by MALS is shown in red over the elution peaks. Schematic representation of the assay setup (**E**). Virion and protein models were generated with PDBe Molstar from a coarse grain model of the virion (51), the crystal structures of the RBD/ACE-2/B0AT1 complex (PDB ID: 6M17) (42), and a human IgG1 (PDB ID: 1HZH) (52). Data from panels (A)–(D) are representative of two independent experiments.

background (Fig. 2B). Matrix effects were evaluated on serial dilutions of serum, plasma, and nonspecific mAb dilutions with acceptable variation (<20%) over a broad range of concentrations (below 40% serum/plasma and 100 μg/ml mAbs) (Fig. 2C). The neutralization potency of matched serum and plasma samples correlated highly ($\rho = 0.9641$, $p < 0.0001$, $n = 108$) (Fig. 2D). Heat inactivation of serum and addition of EDTA had no significant effect (Supplemental Fig. 1). The intra- and interassay CV were found to be satisfactory (4.21% and 12.95%, respectively). Altogether, these results demonstrate that the ELISA-based neutralization test is robust, time-effective, and suitable for the assessment of the neutralization potency in clinical samples.

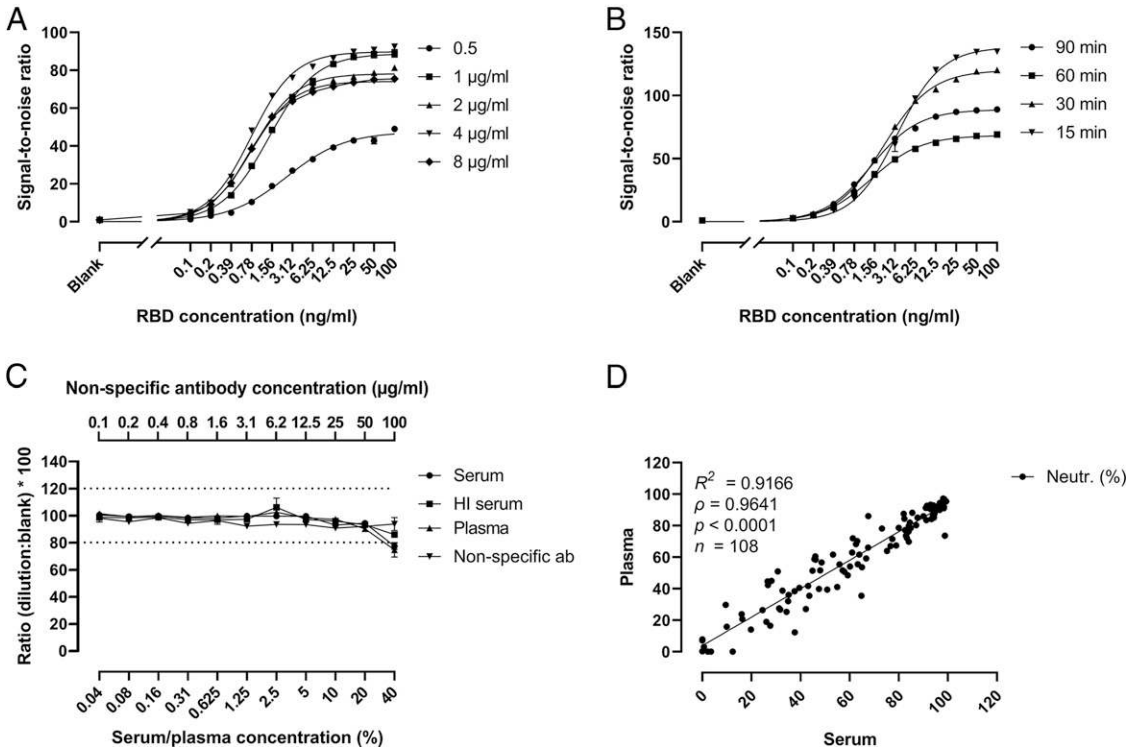

FIGURE 2. Assay development. Signal-to-noise ratio, calculated as the ratio between a given dilution and the blank, of the binding of serial dilutions of RBD on a 2-fold titration of coated ACE-2 (0.5–8 µg/ml) (**A**). Signal-to-noise ratio of the binding of serial dilutions of RBD incubated for 15 to 90 min on plates coated with 1 µg/ml of ACE-2 (**B**). The matrix effects were analyzed by coincubating RBD/HS-strep-HRP in increasing concentrations of a control serum, plasma, or nonspecific Ab pools (**C**). Horizontal dashed lines delimit the 100 ± 20% acceptable recovery range. Spearman rank correlation coefficient between the neutralization (Neutr.) (%) in 20% serum and plasma (**D**). Trend line represents the linear regression (R^2 = 0.9166). Data from panels (A)–(C) are represented as mean ± SEM of duplicate measurements.

The results of the Ab neutralization ELISA closely match those of the PRNT

We compared the performance of the developed Ab neutralization ELISA with an authentic SARS-CoV-2 viral neutralization assay, the PRNT. When categorizing the samples on low, medium, high, and very high neutralization potencies, as calculated by the PRNT, we observed that the Ab neutralization ELISA results match those obtained by the PRNT (n = 15), with estimated IC_{50} values showing a strong correlation with the PRNT (ρ = 0.9231, n = 12) (Fig. 3). Additionally, we benchmarked our Ab neutralization ELISA with two commercially available ELISA-based kits (n = 52). A similarly satisfactory association was observed with two commercially available neutralization tests (ρ = 0.9263–0.9562, R^2 = 0.8445–0.9232, n = 52) (Supplemental Fig. 2).

The neutralization potency and Ab titers against spike, RBD, and N strongly correlates in COVID-19 convalescent patient sera

Using our ELISA neutralization test, we measured the neutralization potency of serum samples from a cohort of convalescent patients with a confirmed COVID-19 diagnosis by quantitative PCR (n = 310). In parallel, we measured the titers of IgG, IgM, and IgA against RBD, spike, and protein N using a direct ELISA approach (Fig. 4), which was published recently (27). The neutralization potency, expressed as the IC_{50}, was strongly correlated to the IgG titers against RBD and spike (ρ = 0.8291 and 0.8297, respectively; $p < 0.0001$) and to a lesser extent with the IgG titers against protein N (ρ = 0.6471, $p < 0.0001$). Weaker correlations, albeit statistically significant, were found for the IgM and IgA titers against all three viral Ags.

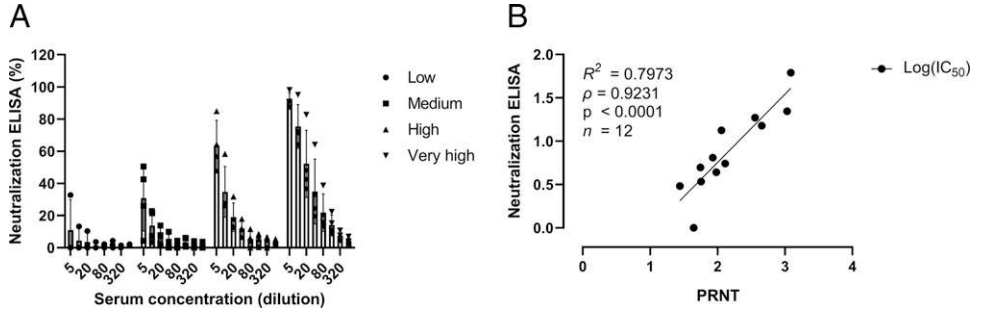

FIGURE 3. Assay validation. The neutralization potency of COVID-19 convalescent patient sera (n = 15) was determined using the PRNT, classified by low, medium, high, and very high neutralization potency, and analyzed using the developed Ab neutralization ELISA (**A**). IC_{50} values were calculated from the neutralization indexes obtained from both tests using the equation [inhibitor] versus normalized response with variable slope, and their relationship was analyzed using linear regression (R^2 = 0.7973) and Spearman rank correlation coefficient (ρ = 0.9231, $p < 0.0001$) (n = 12) (**B**). IC_{50} values could not be interpolated with confidence from "low potency" samples, and as such, were excluded from the correlation.

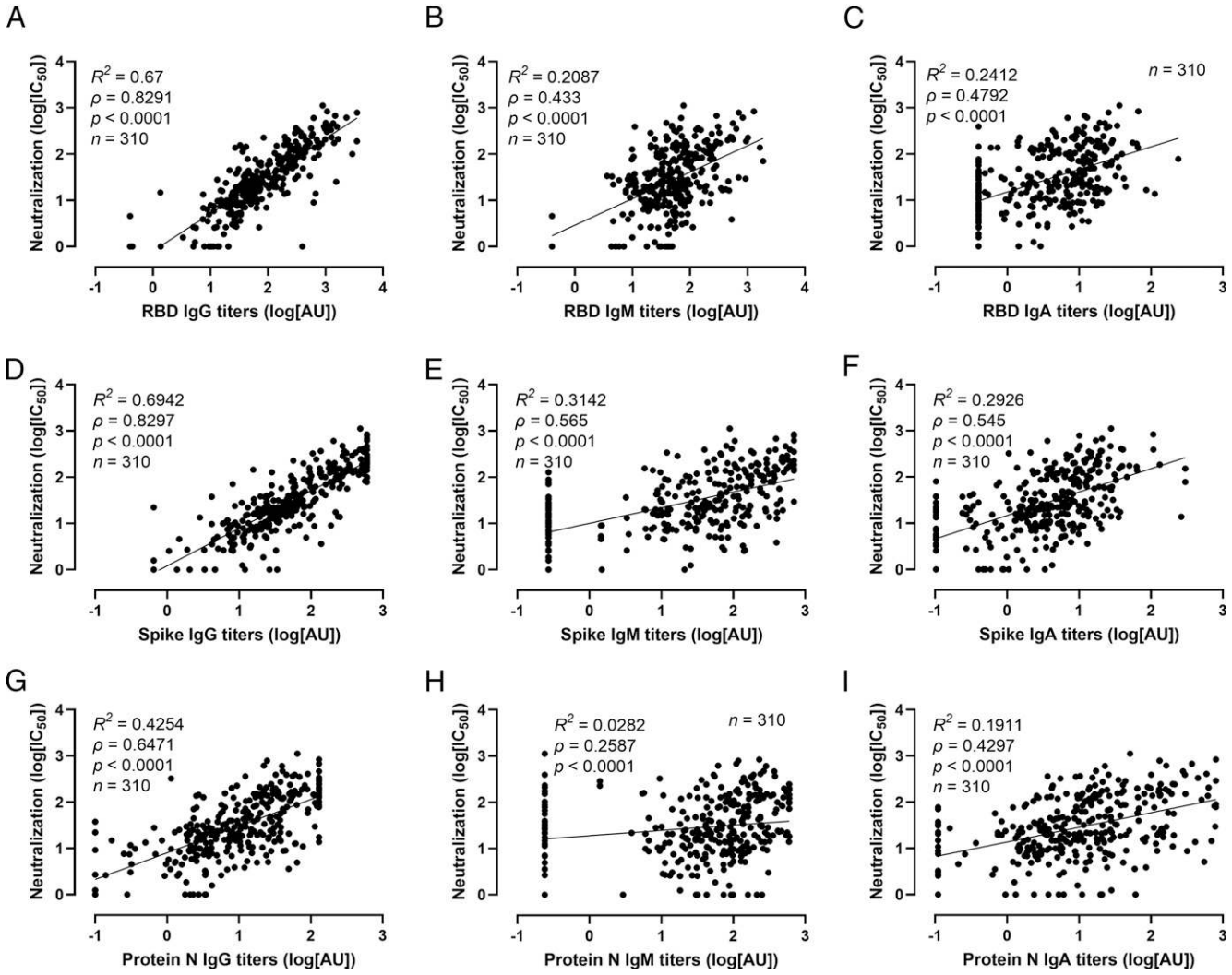

FIGURE 4. Neutralization potency and Ab titers in COVID-19 convalescent patient sera. Spearman rank correlation and linear regression analyses of the neutralization potency of sera and titers of IgG (**A**, **D**, **G**), IgM (**B**, **E**, **H**), and IgA (**C**, **F**, **I**) against RBD (A–C), spike (D–F), and protein N (G–I) (n = 310). Trend lines represent linear regression.

RBD-immunized mice show a more profound neutralization potency than spike-immunized and severe convalescent individuals

Next, we evaluated the Ab response in a preclinical animal vaccine model. Mice were immunized four times s.c. with either the RBD or trimeric spike ectodomain. Each mouse was bled 7 d after the second, third, and fourth immunization followed by an assessment of the polyclonal response against the Ag. The polyclonal Ab titers against RBD and spike from the third immunization round using a direct ELISA are shown in Fig. 5A, 5B. The spike-specific Abs in the RBD and spike-immunized mice groups mirrored each other, whereas the RBD-specific Ab levels were lower in the spike-immunized group. An SARS-CoV-2 nonrelated immunized mouse group was used as a negative control. Compared with the Ab titers developed in COVID-19 convalescent individuals—grouped into high, intermediate, and low titers (as determined by our direct RBD ELISA described above) (Fig. 5C, 5D)—the immunized mice developed in the order of 9- to 32-fold and 20- to 35-fold higher RBD and spike titers, respectively, than any of the convalescent patient groups. Next, we assessed the neutralization potency of immunized mice and convalescent patient sera in our Ab neutralization ELISA (Fig. 5E, 5F), showing that immunized mice, particularly in the RBD group, developed a robust neutralizing response, which was 500-fold more potent than the highest titer response group of convalescent individuals. Ab titers and neutralization potency of mouse sera reached a maximum already after the second round of immunization. The presented data were generated from sera collected after the third immunization.

Murine mAbs display high RBD affinity and strong inhibitory properties

In the light of the promising results with the polyclonal mice sera, we sought to isolate and characterize potent murine mAbs. We selected and characterized 17 mAbs immunized with RBD and 32 mAbs using trimeric full-length trimeric spike protein ectodomain as Ags and a selected group of these were purified by affinity chromatography. All clones isolated from RBD-immunized mice reacted with RBD and spike to the same extent. However, for the clones that originated from spike-immunized mice, only 3 out of 32 mAbs showed full RBD/ACE-2 inhibition, whereas 9 out of 17 of the mAbs from the RBD immunization showed a strong inhibition profile. In the neutralization assessment, we selected mAbs with a high binding capacity to the RBD (a total of three mAbs from the spike and seven from the RBD immunization). These were further characterized in terms of biochemical and neutralization properties (Fig. 6). First, we studied their binding properties using BLI (Fig. 6A, 6B). The mAbs were immobilized onto biosensor tips and dipped into wells containing 2-fold dilution series of RBD (0.4–200 nM). All Abs bound to RBD with low nM (n = 4) or sub nM affinity (n = 5). Epitope binning experiments revealed several epitope

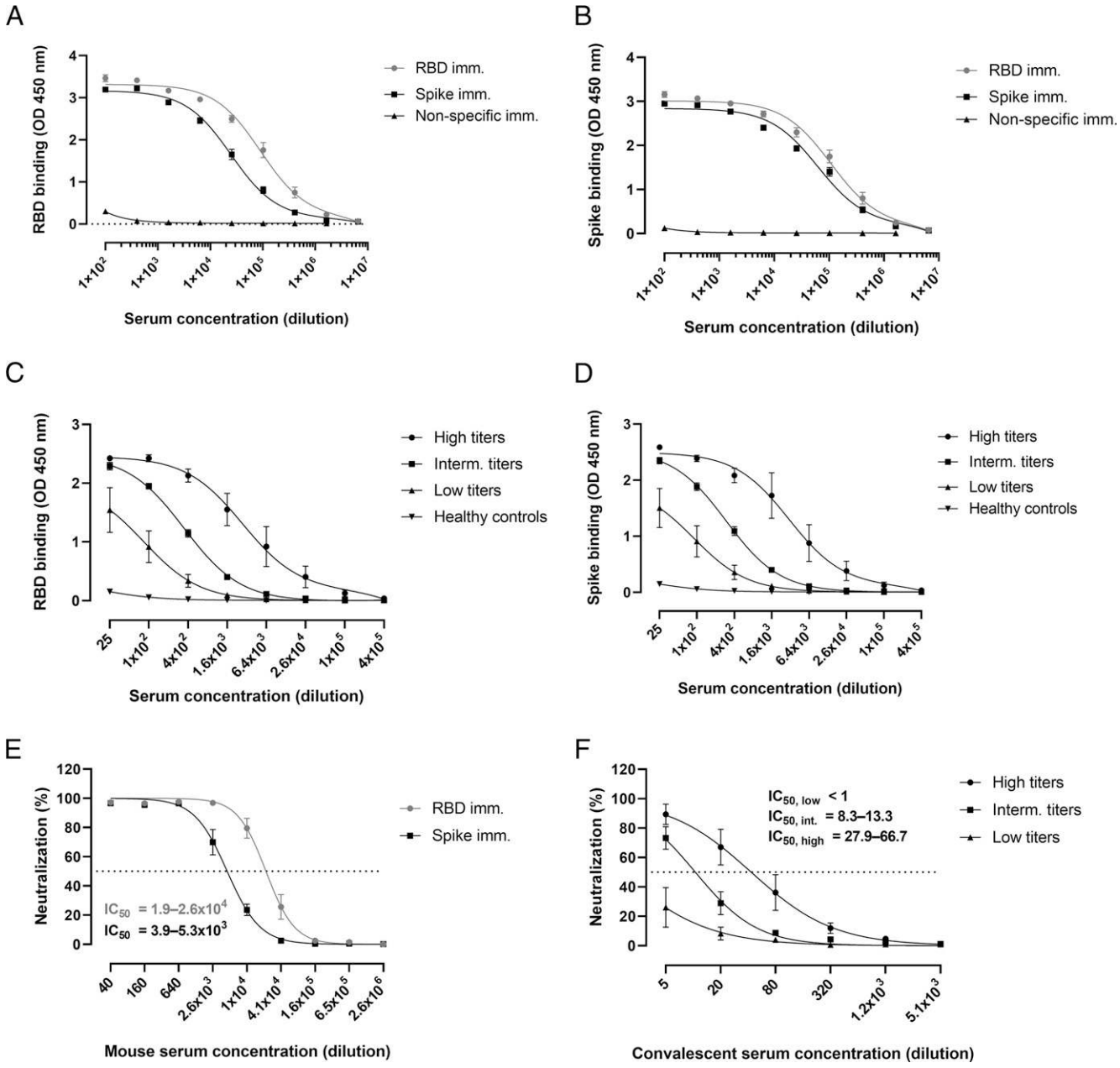

FIGURE 5. Ab titers and neutralization potency of polyclonal mouse and convalescent patient sera. Plates coated with recombinant RBD (**A**, **C**) or spike ectodomain (**B**, **D**). Mouse sera from mice immunized with RBD (RBD imm.), spike (Spike imm.), or a SARS-CoV-2 nonrelated Ag (Nonspecific imm.) applied in a 4-fold dilution ($n = 4$ per group) (A, B). Human convalescent sera with high, intermediate, and low RBD-specific IgG titers were applied in a 4-fold dilution ($n = 4$ per group) (C, D). Serum samples from healthy blood donors were used as negative controls ($n = 4$). Neutralization potency of polyclonal sera from mice immunized with RBD (RBD. imm.) or spike ectodomain (Spike imm.) using our Ab neutralization ELISA ($n = 4$ per group) (**E**). Connecting lines represent a nonlinear fit using the equation one site – total binding. Neutralization potency of human convalescent sera grouped by RBD-specific IgG titers ($n = 5$ per group) (**F**). Connecting lines represent a nonlinear fit using the equation [inhibitor] versus normalized response with variable slope. Data are presented as mean ± SEM. IC_{50} values are reported as 95% asymmetrical confidence intervals.

hotspots within the RBD, one recognized by RBD clones 1 and 28, and a second recognized by four RBD (15, 26, 30, 31) and one spike clones (53), with RBD clone 5 partially overlapping the same region of RBD clone 15 (Fig. 6B). A third region was located in the spike protein and did not appear to be involved in the interaction with the ACE-2 receptor. Next, we assessed the neutralization potency of the mAbs both in the PRNT (Fig. 6C) and in the Ab neutralization ELISA (Fig. 6D). In Fig. 6C, 6D, 3 mAbs are illustrated (i.e., two targeting a common epitope within the RBD, and one outside). All seven RBD mAbs were neutralizing, with IC_{50} values ranging from 2 to 20 μg/ml. Of the three spike mAbs, the two mapping outside the RBD were nonneutralizing, whereas spike clone 53 outperformed all others with an estimated IC_{50} of 0.2–0.3 μg/ml. Binding affinities toward RBD (K_d) were not directly correlated with neutralization potency (Fig. 6D).

Discussion

There is an urgent need for relevant serological assays to measure the protective effects of the emerging SARS-CoV-2 vaccines. To monitor the prevalence of SARS-CoV-2–exposed individuals in a population, many assays are based either on direct detection of antiviral Abs or employing an indirect principle using viral Ags both for capture and detection (33–36; B. Isho, K. T. Abe, M. Zuo, A. J. Jamal, B. Rathod, J. H. Wang, Z. Li, G. Chao, O. L. Rojas, Y. M.

A

MAb clone	K_d (M)	Ka (1/Ms)	Kdis (1/s)
RBD 1	1.36 x10^{-10}	6.19 x10^{6}	8.4 x10^{-4}
RBD 5	3.36 x10^{-9}	1.05 x10^{6}	3.53 x10^{-3}
RBD 15	2.36 x10^{-9}	7.23 x10^{5}	1.71 x10^{-3}
RBD 26	7.19 x10^{-10}	4.34 x10^{5}	3.12 x10^{-4}
RBD 28	1.44 x10^{-10}	2.2 x10^{6}	3.17 x10^{-4}
RBD 30	5.29 x10^{-10}	1.69 x10^{6}	8.95 x10^{-4}
RBD 31	1.84 x10^{-9}	1.86 x10^{5}	3.42 x10^{-4}
Spike 43	-	-	-
Spike 53	2.8 x10^{-10}	3.66 x10^{5}	1.04 x10^{-4}
Spike 56	2.06 x10^{-9}	1.31 x10^{5}	2.70 x10^{-4}

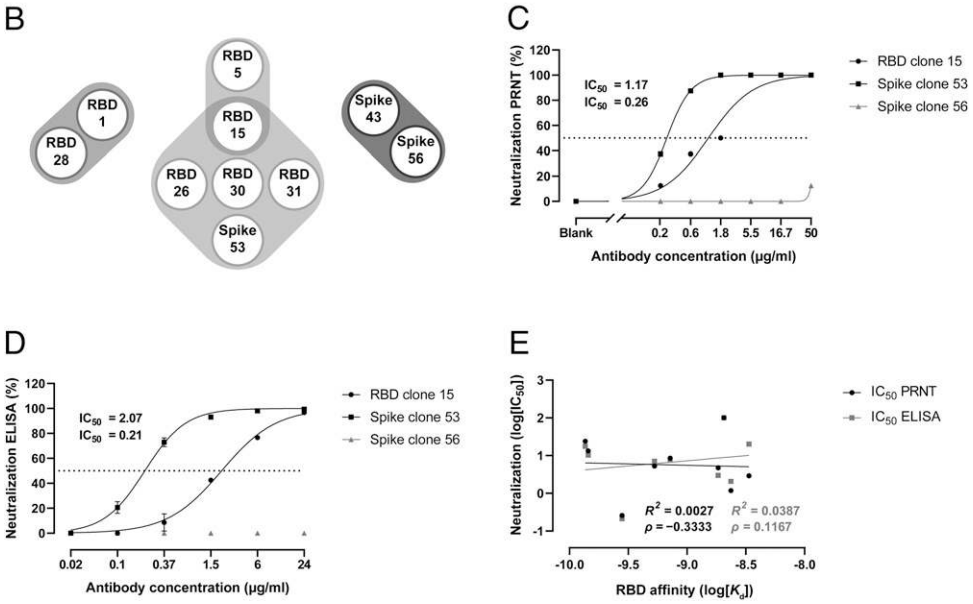

FIGURE 6. Characterization of SARS-CoV-2 neutralizing mAbs. Binding kinetics of selected mAbs isolated from RBD or spike-immunized mice were determined by BLI (**A**). The Abs were immobilized in AMC sensors and dipped into serial dilutions of RBD (10-point 2-fold dilution starting at 200 nM). Epitope binning experiments on monomeric spike protein via BLI identified two noncompeting epitopes for both RBD and spike (**B**). The neutralization potency of three representative high-affinity mAbs was estimated by the PRNT (**C**) and the Ab neutralization ELISA (**D**) (n = 1). Correlation between the neutralization potencies calculated by the PRNT and the Ab neutralization ELISA-based test and the dissociation constant (K_d) calculated by BLI (**E**). Best-fit IC_{50} values from nonneutralizing mAbs were normalized to 100. Nonneutralizing spike clone 43 was excluded from the analysis. Trend line represents the linear regression. Data from panel (D) are represented as mean ± SEM of duplicate measurements.

Bang, et al., manuscript posted on medRxiv, DOI: 10.1101/2020.08.01.20166553). However, none of these assays measures whether an exposed individual has developed neutralizing protective Abs. A good alternative would be the PRNT assays. They are considered the gold standard for the evaluation of neutralizing Ab titers. However, PRNT assays are time-consuming, require high-class biosafety laboratories, have low output, and are expensive to perform (18–21). Because the viral entry of the SARS-CoV-2 to the target cell requires interaction between the RBD domain and the host ACE-2 receptor (30, 37, 38), we have developed a fast and simple Ab neutralization ELISA as a proxy for viral neutralization. Using recombinant ectodomains of ACE-2 as capture and biotinylated RBD for detection we were able to establish an Ab inhibition ELISA that correlated highly (ρ = 0.9231, $p < 0.0001$) with the PRNT assay using COVID-19 convalescent sera with a titer spectrum of anti–SARS-CoV-2 Abs. This suggests that the newly developed Ab neutralization ELISA could replace PRNT and similar assays as a proxy tool to measure Ab-dependent SARS-CoV-2 neutralization. The assay was robust and could be used with various types of analytes (plasma, serum, heat-inactivated serum, and purified mAb preparations). Moreover, we could show that the Ab neutralization ELISA correlated well with similar newly launched commercial assays to evaluate viral neutralization. Interestingly, the Ab neutralization ELISA showed a good correlation with IgG Ab levels against SARS-CoV-2 RBD, full-length spike, and protein N, but only a modest correlation with IgA and IgM levels, in agreement with other reports (39).

To mimic a vaccine situation, we tested the ability of the Ab neutralization ELISA to assess the inhibition capacity of sera from mice vaccinated with either recombinant trimeric spike ectodomain or RBD. The spike ectodomain was confirmed to behave as a trimer in solution by SEC-MALS, with a major peak with a calculated mass of 530 kDa, and a small shoulder corresponding to a dimer of trimers. The difference between theoretical (411 kDa) and measured molar mass (530 kDa) likely results from heavy glycosylation of the spike protein (40). We performed four rounds of immunization and observed that Ab levels against RBD and spike, as well as neutralization potency, reached a maximum already after the second round (data not shown), indicating that two immunizations with 14-d intervals are sufficient to develop a potent adaptive humoral response. We observed a clear difference in terms of IC_{50} between the neutralization potency of RBD and full-length spike protein–immunized mice sera; a much better neutralizing capacity was observed when RBD was used as the immunogen. The reason for this is unknown at present. Our vaccine regimen using the same mass of Ags (20 µg/immunization) entailed an approximate 4.5-fold difference in "presented RBD units" (i.e., 176 kDa spike monomer versus 39 kDa RBD). Considering that the RBD is central in the virus interaction with the human ACE-2 receptor (41), and in light of the observations that the RBD is one of the main targets of neutralizing Abs (11–13, 42–44), we propose that immunizing with RBD alone will generate an Ab response where a greater fraction of the Abs will be neutralizing compared with the full spike. Moreover, our results could imply that the BCR epitope repertoire is highly distributed on the spike protein surface, leading to a greater fraction of nonneutralizing Abs that are either nonfunctional or deleterious—Abs that bind to viral Ags without blocking infection may exacerbate disease severity in a process known as Ab-dependent enhancement (ADE) (45, 46). Vaccine-induced ADE has been reported in animal models immunized with a viral vector expressing the SARS-CoV spike

protein (47), as well as peptide epitopes of the SARS-CoV spike (48), although there is no evidence of vaccine- or infection-mediated ADE in COVID-19 to date. Nonetheless, a focused immunization approach using only the RBD might be relevant to consider in future vaccine development strategies. Compatible with such notion is our observation that sera from convalescent individuals that have been exposed to the whole virus had several hundred–fold less neutralizing capacity than the mice immunized with RBD. However, some caution should be taken because we do not know whether the mice response can be directly translated to the human situation. Nevertheless, the results suggest that the RBD without any carrier or other specific formulations could be an excellent vaccine candidate.

To further address whether the Ab neutralization ELISA could be used to monitor mAb therapeutics, we developed a panel of mAbs raised against either trimeric ectodomain spike or RBD. These results show that most of the mAbs raised against RBD were indeed virus-neutralizing (9 out of 17 with a full inhibition and 5 showed a partial inhibition profile), whereas a minority of the total number of spike-raised mAbs neutralized the virus (3 out of 32). The mAbs that proved to be of very high affinity (low nM to sub nM KDs) could furthermore be a relevant therapeutic platform to pursue as a neutralizing engineered single-chain variable fragment mAb pool capable of inhibiting viral entry without exacerbating the inflammatory response. Moreover, mixtures of noncompeting mAbs can broaden the efficacy of Ab-based treatments by preventing the appearance of potential escape variants, as seen in other viral diseases such as SARS-CoV-1 (49) and HIV (50), and providing universal coverage of circulating SARS-CoV-2 isolates.

In conclusion, we have developed a platform to monitor the neutralizing capacity of convalescent plasma meant for COVID-19 therapy, that because of its ease of use and safety, could be used in hospitals without access to biosafety level 3 laboratories as a routine test before and after plasmapheresis. Moreover, it can be used as an easy screening platform for selecting the most suitable mAbs for therapeutic development. Probably more important, our platform can be used to monitor the neutralizing humoral vaccine responses toward SARS-Cov-2 safely and on a large scale. Moreover, our data suggest that using RBD as an immunogen compared with full-length spike protein might be a better strategy in creating a robust neutralization Ab response. This should be considered when developing next-generation vaccines against SARS-CoV-2 or related escape strains that could potentially emerge after the present pandemic.

Acknowledgments

The authors thank Jette Thorsen (Department of Biophysics and Injectable Formulation 2, Novo Nordisk) and Mads Ole Nymand Dam (Department of Antibody Technology, Novo Nordisk) for expert laboratory assistance. The authors also thank Camilla Xenia Holtermann Jahn, Sif Kaas Nielsen, and Jytte Bryde Clausen (Laboratory of Molecular Medicine, Copenhagen University Hospital) for excellent technical assistance.

Disclosures

The authors have no financial conflicts of interest.

References

1. Le, T. T., J. P. Cramer, R. Chen, and S. Mayhew. 2020. Evolution of the COVID-19 vaccine development landscape. *Nat. Rev. Drug Discov.* 19: 667–668.
2. World Health Organization. 2021. Coronavirus disease (COVID-19): Vaccines Q&A. Available at: https://www.who.int/news-room/q-a-detail/coronavirus-disease-(covid-19)-vaccines.
3. Sajna, K. V., and S. Kamat. 2021. Antibodies at work in the time of severe acute respiratory syndrome coronavirus 2. *Cytotherapy* 23: 101–110.
4. Thevarajan, I., T. H. O. Nguyen, M. Koutsakos, J. Druce, L. Caly, C. E. van de Sandt, X. Jia, S. Nicholson, M. Catton, B. Cowie, et al. 2020. Breadth of concomitant immune responses prior to patient recovery: a case report of non-severe COVID-19. *Nat. Med.* 26: 453–455.
5. Ni, L., F. Ye, M.-L. Cheng, Y. Feng, Y.-Q. Deng, H. Zhao, P. Wei, J. Ge, M. Gou, X. Li, et al. 2020. Detection of SARS-CoV-2-specific humoral and cellular immunity in COVID-19 convalescent individuals. *Immunity* 52: 971–977.e3.
6. Suthar, M. S., M. G. Zimmerman, R. C. Kauffman, G. Mantus, S. L. Linderman, W. H. Hudson, A. Vanderheiden, L. Nyhoff, C. W. Davis, O. Adekunle, et al. 2020. Rapid generation of neutralizing antibody responses in COVID-19 patients. *Cell Rep. Med.* 1: 100040.
7. Long, Q.-X., X.-J. Tang, Q.-L. Shi, Q. Li, H.-J. Deng, J. Yuan, J.-L. Hu, W. Xu, Y. Zhang, F.-J. Lv, et al. 2020. Clinical and immunological assessment of asymptomatic SARS-CoV-2 infections. *Nat. Med.* 26: 1200–1204.
8. Wang, X., X. Guo, Q. Xin, Y. Pan, Y. Hu, J. Li, Y. Chu, Y. Feng, and Q. Wang. 2020. Neutralizing antibody responses to severe acute respiratory syndrome coronavirus 2 in coronavirus disease 2019 inpatients and convalescent patients. *Clin. Infect. Dis.* 71: 2688–2694.
9. Zost, S. J., P. Gilchuk, J. B. Case, E. Binshtein, R. E. Chen, J. P. Nkolola, A. Schäfer, J. X. Reidy, A. Trivette, R. S. Nargi, et al. 2020. Potently neutralizing and protective human antibodies against SARS-CoV-2. *Nature* 584: 443–449.
10. Lv, Z., Y.-Q. Deng, Q. Ye, L. Cao, C.-Y. Sun, C. Fan, W. Huang, S. Sun, Y. Sun, L. Zhu, et al. 2020. Structural basis for neutralization of SARS-CoV-2 and SARS-CoV by a potent therapeutic antibody. *Science* 369: 1505–1509.
11. Wu, Y., F. Wang, C. Shen, W. Peng, D. Li, C. Zhao, Z. Li, S. Li, Y. Bi, Y. Yang, et al. 2020. A noncompeting pair of human neutralizing antibodies block COVID-19 virus binding to its receptor ACE2. *Science* 368: 1274–1278.
12. Liu, L., P. Wang, M. S. Nair, J. Yu, M. Rapp, Q. Wang, Y. Luo, J. F.-W. Chan, V. Sahi, A. Figueroa, et al. 2020. Potent neutralizing antibodies against multiple epitopes on SARS-CoV-2 spike. *Nature* 584: 450–456.
13. Cao, Y., B. Su, X. Guo, W. Sun, Y. Deng, L. Bao, Q. Zhu, X. Zhang, Y. Zheng, C. Geng, et al. 2020. Potent neutralizing antibodies against SARS-CoV-2 identified by high-throughput single-cell sequencing of convalescent patients' B cells. *Cell* 182: 73–84.e16.
14. National Institutes of Health. 2021. Anti-SARS-CoV-2 monoclonal antibodies. https://www.covid19treatmentguidelines.nih.gov/anti-sars-cov-2-antibody-products/.
15. Chen, P., A. Nirula, B. Heller, R. L. Gottlieb, J. Boscia, J. Morris, G. Huhn, J. Cardona, B. Mocherla, V. Stosor, et al. BLAZE-1 Investigators. 2021. SARS-CoV-2 neutralizing antibody LY-CoV555 in outpatients with Covid-19. *N. Engl. J. Med.* 384: 229–237.
16. Simonovich, V. A., L. D. Burgos Pratx, P. Scibona, M. V. Beruto, M. G. Vallone, C. Vázquez, N. Savoy, D. H. Giunta, L. G. Pérez, M. D. L. Sánchez, et al. PlasmAr Study Group. 2021. A randomized trial of convalescent plasma in Covid-19 severe pneumonia. *N. Engl. J. Med.* 384: 619–629.
17. Libster, R., G. Pérez Marc, D. Wappner, S. Coviello, A. Bianchi, V. Braem, I. Esteban, M. T. Caballero, C. Wood, M. Berrueta, et al. Fundación INFANT–COVID-19 Group. 2021. Early high-titer plasma therapy to prevent severe Covid-19 in older adults. *N. Engl. J. Med.* 384: 610–618.
18. Ward, B. J., S. Aouchiche, N. Martel, F. M. Bertley, N. Bautista-Lopez, B. Serhir, and S. Ratnam. 1999. Measurement of measles virus-specific neutralizing antibodies: evaluation of the syncytium inhibition assay in comparison with the plaque reduction neutralization test. *Diagn. Microbiol. Infect. Dis.* 33: 147–152.
19. Ratnam, S., V. Gadag, R. West, J. Burris, E. Oates, F. Stead, and N. Bouilianne. 1995. Comparison of commercial enzyme immunoassay kits with plaque reduction neutralization test for detection of measles virus antibody. *J. Clin. Microbiol.* 33: 811–815.
20. Mauldin, J., K. Carbone, H. Hsu, R. Yolken, and S. Rubin. 2005. Mumps virus-specific antibody titers from pre-vaccine era sera: comparison of the plaque reduction neutralization assay and enzyme immunoassays. *J. Clin. Microbiol.* 43: 4847–4851.
21. Gonçalves, G., F. Cutts, T. Forsey, and H. R. Andrade. 1999. Comparison of a commercial enzyme immunoassay with plaque reduction neutralization for maternal and infant measles antibody measurement. *Rev. Inst. Med. Trop. São Paulo* 41: 21–26.
22. Yang, R., B. Huang, R. A, W. Li, W. Wang, Y. Deng, and W. Tan. 2020. Development and effectiveness of pseudotyped SARS-CoV-2 system as determined by neutralizing efficiency and entry inhibition test *in vitro*. *Biosaf. Health* 2: 226–231.
23. Johnson, M. C., T. D. Lyddon, R. Suarez, B. Salcedo, M. LePique, M. Graham, C. Ricana, C. Robinson, and D. G. Ritter. 2020. Optimized pseudotyping conditions for the SARS-COV-2 spike glycoprotein. *J. Virol.* 94: e01062-20.
24. Schmidt, F., Y. Weisblum, F. Muecksch, H.-H. Hoffmann, E. Michailidis, J. C. C. Lorenzi, P. Mendoza, M. Rutkowska, E. Bednarski, C. Gaebler, et al. 2020. Measuring SARS-CoV-2 neutralizing antibody activity using pseudotyped and chimeric viruses. *J. Exp. Med.* 217: e20201181.
25. Case, J. B., P. W. Rothlauf, R. E. Chen, Z. Liu, H. Zhao, A. S. Kim, L.-M. Bloyet, Q. Zeng, S. Tahan, L. Droit, et al. 2020. Neutralizing antibody and soluble ACE2 inhibition of a replication-competent VSV-SARS-CoV-2 and a clinical isolate of SARS-CoV-2. *Cell Host Microbe.* 28: 475–485.e5.
26. Xiong, H.-L., Y.-T. Wu, J.-L. Cao, R. Yang, Y.-X. Liu, J. Ma, X.-Y. Qiao, X.-Y. Yao, B.-H. Zhang, Y.-L. Zhang, et al. 2020. Robust neutralization assay based on SARS-CoV-2 S-protein-bearing vesicular stomatitis virus (VSV) pseudovirus and ACE2-overexpressing BHK21 cells. *Emerg. Microbes Infect.* 9: 2105–2113.
27. Hansen, C. B., I. Jarlhelt, L. Pérez-Alós, L. Hummelshøj Landsy, M. Loftager, A. Rosbjerg, C. Helgstrand, J. R. Bjelke, T. Egebjerg, J. G. Jardine, et al. 2020.

SARS-CoV-2 antibody responses are correlated to disease severity in COVID-19 convalescent individuals. *J. Immunol.* 206: 109–117.
28. Wrapp, D., N. Wang, K. S. Corbett, J. A. Goldsmith, C.-L. Hsieh, O. Abiona, B. S. Graham, and J. S. McLellan. 2020. Cryo-EM structure of the 2019-nCoV spike in the prefusion conformation. *Science* 367: 1260–1263.
29. Jung, S.-K., and K. McDonald. 2011. Visual gene developer: a fully programmable bioinformatics software for synthetic gene optimization. *BMC Bioinformatics* 12: 340.
30. Hoffmann, M., H. Kleine-Weber, S. Schroeder, N. Krüger, T. Herrler, S. Erichsen, T. S. Schiergens, G. Herrler, N.-H. Wu, A. Nitsche, et al. 2020. SARS-CoV-2 cell entry depends on ACE2 and TMPRSS2 and is blocked by a clinically proven protease inhibitor. *Cell* 181: 271–280.e8.
31. Reed, L. J., and H. Muench. 1938. A simple method of estimating fifty percent endpoints. *Am. J. Epidemiol.* 27: 493–497.
32. Skjoedt, M.-O., Y. Palarasah, K. Rasmussen, L. Vitved, J. Salomonsen, A. Kliem, S. Hansen, C. Koch, and K. Skjodt. 2010. Two mannose-binding lectin homologues and an MBL-associated serine protease are expressed in the gut epithelia of the urochordate species Ciona intestinalis. *Dev. Comp. Immunol.* 34: 59–68.
33. Luchsinger, L. L., B. P. Ransegnola, D. K. Jin, F. Muecksch, Y. Weisblum, W. Bao, P. J. George, M. Rodriguez, N. Tricoche, F. Schmidt, et al. 2020. Serological assays estimate highly variable SARS-CoV-2 neutralizing antibody activity in recovered COVID-19 patients. *J. Clin. Microbiol.* 58: e02005-20.
34. Okba, N. M. A., M. A. Müller, W. Li, C. Wang, C. H. GeurtsvanKessel, V. M. Corman, M. M. Lamers, R. S. Sikkema, E. de Bruin, F. D. Chandler, et al. 2020. Severe acute respiratory syndrome coronavirus 2-specific antibody responses in coronavirus disease patients. *Emerg. Infect. Dis.* 26: 1478–1488.
35. Amanat, F., D. Stadlbauer, S. Strohmeier, T. H. O. Nguyen, V. Chromikova, M. McMahon, K. Jiang, G. A. Arunkumar, D. Jurczyszak, J. Polanco, et al. 2020. A serological assay to detect SARS-CoV-2 seroconversion in humans. *Nat. Med.* 26: 1033–1036.
36. Wang, Y., L. Zhang, L. Sang, F. Ye, S. Ruan, B. Zhong, T. Song, A. N. Alshukairi, R. Chen, Z. Zhang, et al. 2020. Kinetics of viral load and antibody response in relation to COVID-19 severity. *J. Clin. Invest.* 130: 5235–5244.
37. Zhou, P., X. L. Yang, X.-G. G. Wang, B. Hu, L. Zhang, W. Zhang, H.-R. R. Si, Y. Zhu, B. Li, C.-L. L. Huang, et al. 2020. A pneumonia outbreak associated with a new coronavirus of probable bat origin. *Nature* 579: 270–273.
38. Walls, A. C., Y.-J. J. Park, M. A. Tortorici, A. Wall, A. T. McGuire, and D. Veesler. 2020. Structure, function, and antigenicity of the SARS-CoV-2 spike glycoprotein. [Published erratum appears in 2020 *Cell* 183: 1735]. *Cell* 181: 281–292.e6.
39. Bošnjak, B., S. C. Stein, S. Willenzon, A. K. Cordes, W. Puppe, G. Bernhardt, I. Ravens, C. Ritter, C. R. Schultze-Florey, N. Gödecke, et al. 2020. Low serum neutralizing anti-SARS-CoV-2 S antibody levels in mildly affected COVID-19 convalescent patients revealed by two different detection methods. *Cell. Mol. Immunol.* 18: 936–944.
40. Watanabe, Y., J. D. Allen, D. Wrapp, J. S. McLellan, and M. Crispin. 2020. Site-specific glycan analysis of the SARS-CoV-2 spike. *Science* 369: 330–333.
41. Yan, R., Y. Zhang, Y. Li, L. Xia, Y. Guo, and Q. Zhou. 2020. Structural basis for the recognition of SARS-CoV-2 by full-length human ACE2. *Science* 367: 1444–1448.
42. Brouwer, P. J. M., T. G. Caniels, K. van der Straten, J. L. Snitselaar, Y. Aldon, S. Bangaru, J. L. Torres, N. M. A. Okba, M. Claireaux, G. Kerster, et al. 2020. Potent neutralizing antibodies from COVID-19 patients define multiple targets of vulnerability. *Science* 369: 643–650.
43. Shi, R., C. Shan, X. Duan, Z. Chen, P. Liu, J. Song, T. Song, X. Bi, C. Han, L. Wu, et al. 2020. A human neutralizing antibody targets the receptor-binding site of SARS-CoV-2. *Nature* 584: 120–124.
44. Wan, J., S. Xing, L. Ding, Y. Wang, C. Gu, Y. Wu, B. Rong, C. Li, S. Wang, K. Chen, et al. 2020. Human-IgG-neutralizing monoclonal antibodies block the SARS-CoV-2 infection. *Cell Rep.* 32: 107918.
45. Lee, W. S., A. K. Wheatley, S. J. Kent, and B. J. DeKosky. 2020. Antibody-dependent enhancement and SARS-CoV-2 vaccines and therapies. *Nat. Microbiol.* 5: 1185–1191.
46. Arvin, A. M., K. Fink, M. A. Schmid, A. Cathcart, R. Spreafico, C. Havenar-Daughton, A. Lanzavecchia, D. Corti, and H. W. Virgin. 2020. A perspective on potential antibody-dependent enhancement of SARS-CoV-2. *Nature* 584: 353–363.
47. Liu, L., Q. Wei, Q. Lin, J. Fang, H. Wang, H. Kwok, H. Tang, K. Nishiura, J. Peng, Z. Tan, et al. 2019. Anti-spike IgG causes severe acute lung injury by skewing macrophage responses during acute SARS-CoV infection. *JCI Insight* 4: e123158.
48. Wang, Q., L. Zhang, K. Kuwahara, L. Li, Z. Liu, T. Li, H. Zhu, J. Liu, Y. Xu, J. Xie, et al. 2016. Immunodominant SARS coronavirus epitopes in humans elicited both enhancing and neutralizing effects on infection in non-human primates. *ACS Infect. Dis.* 2: 361–376.
49. ter Meulen, J., E. N. van den Brink, L. L. M. Poon, W. E. Marissen, C. S. W. Leung, F. Cox, C. Y. Cheung, A. Q. Bakker, J. A. Bogaards, E. van Deventer, et al. 2006. Human monoclonal antibody combination against SARS coronavirus: synergy and coverage of escape mutants. *PLoS Med.* 3: e237.
50. Caskey, M., T. Schoofs, H. Gruell, A. Settler, T. Karagounis, E. F. Kreider, B. Murrell, N. Pfeifer, L. Nogueira, T. Y. Oliveira, et al. 2017. Antibody 10-1074 suppresses viremia in HIV-1-infected individuals. *Nat. Med.* 23: 185–191.
51. Yu, A., A. J. Pak, P. He, V. Monje-Galvan, L. Casalino, Z. Gaieb, A. C. Dommer, R. E. Amaro, and G. A. Voth. 2020. A multiscale coarse-grained model of the SARS-CoV-2 virion. *Biophys. J.* 120: 1097–1104.
52. Saphire, E. O., P. W. Parren, R. Pantophlet, M. B. Zwick, G. M. Morris, P. M. Rudd, R. A. Dwek, R. L. Stanfield, D. R. Burton, and I. A. Wilson. 2001. Crystal structure of a neutralizing human IGG against HIV-1: a template for vaccine design. *Science* 293: 1155–1159.